Arabian Journal of Chemistry (2021) **14**, 103043

King Saud University

Arabian Journal of Chemistry

www.ksu.edu.sa
www.sciencedirect.com

ORIGINAL ARTICLE

Production of the complete fertilizer with simultaneously removing sulfur oxides and nitrogen oxides using yellow phosphorus

Montaser Abduallah Mohammed Alzaky [a,b,*], **Dengxin Li** [b]

[a] *College of Chemistry, Chemical Engineering, and Biotechnology, DongHua University, Shanghai 201620, China*
[b] *College of Environmental Science and Engineering, DongHua University, Shanghai 201620, China*

Received 15 September 2020; accepted 21 January 2021
Available online 2 February 2021

KEYWORDS

NPK;
SO_2 Removal;
NO Removal;
Flue Gas;
White/Yellow phosphorus

Abstract Flue gases proved to have several human and environmental problems. Although they are many, SO_X and NO_X are the most famous, due to their direct human, animal, and plant effect. Thus, their removal represents one of the main concerns worldwide. Whereas there are several available techniques for this task, herein we applied a unique method through the white/yellow phosphorus (P_4). Our target was to achieve the simultaneous removal together with obtaining the complete fertilizer Nitrogen, Phosphorus, Potassium (NPK). The removal efficiency investigated with and without the ozone, SO_X and NO_X removal reach 100% at a faster time with the ozone existence. Also, examining the optimal P_4 weight that was 0.5 g, furthermore, the optimum stirring intensity proves to be 1083 rpm, additionally, the optimum temperature was 55 °C, finally, it was compared with the most famous absorbers. The system efficiency was tested in a special experiment, furthermore, the reaction mechanism was identified together with testing the solid precipitate using Raman spectroscopy and X-Ray Diffraction (XRD).

© 2021 Published by Elsevier B.V. on behalf of King Saud University. This is an open access article under the CC BY-NC-ND license (http://creativecommons.org/licenses/by-nc-nd/4.0/).

1. Introduction

Recently, fossil fuel combustion had increased severely in different aspects, which represent the main SO_X and NO_X emissions source, typically, the fossil fuel plants are responsible for 87% of the SO_X emissions, and 67% of the NO_X emissions. They are gaining increasing attention because they can be suspended in the atmosphere, therefore, causing several problems, such as acid rains, fog, photochemical smog, and several human respiratory problems (Hsu et al., 2007; Joseph Alcamo, 1987; Bernard, 2001).

---

* Address: College of Environmental Science and Engineering, DongHua University, Shanghai, China (M.A.M. Alzaky).
E-mail addresses: montaserabduallah@hotmail.com (M.A.M. Alzaky), lidengxin@dhu.edu.cn (D. Li).

Peer review under responsibility of King Saud University.

ELSEVIER Production and hosting by Elsevier

https://doi.org/10.1016/j.arabjc.2021.103043
1878-5352 © 2021 Published by Elsevier B.V. on behalf of King Saud University.
This is an open access article under the CC BY-NC-ND license (http://creativecommons.org/licenses/by-nc-nd/4.0/).

Normally, SO_X removed using Flue Gas Desulfurization (FGD) techniques, which apply limestone to neutralize SO_X to sulfur compounds and produce gypsum as a byproduct. On the other hand, for NO_X the FGD isn't effective, rather the Selective Catalytic Reduction (SCR) is applied for it. Traditionally, the simultaneous removal for both of them, obtained through installing FGD and SCR units in series, but recently the research is directed toward one unit that does the simultaneous removal. As SO_2 represents 95% to 98% of SO_X and NO represents 90% to 95% of NO_X, usually, SO_2 and NO refer to SO_X and NO_X respectively. Generally, the fossil fuel burning is through the air as O_2 carriers, but it also means 79% of the air which is N_2 will emerge out as a byproduct, therefore, NO_X always the biggest amount and the main burden. Moreover, the majority of the techniques are using water, consequently, solubility is an important factor. Herein, as SO_2 is soluble, NO isn't and needs to be oxidized then absorbed later. This can be achieved in several ways, such as oxidants (H_2O_2, O_3, $KMnO_4$, etc.), Iron Ⅱ chelates, or other oxidation methods. Although there are numerous techniques available for the simultaneous removal, the widest is the Wet Oxidation Absorption WOA, in which the NO is oxidized then absorbed at the same time with SO_2 (Liu and Chang, 1991; Shuai Li, 2018).

Yellow phosphorus is one of the promising elements for SO_X and NO_X simultaneous removal, which has the ability to generate ozone that can oxidize NO, hence get rid of the oxidants and their cost. Moreover, it offers excellent SO_X abatement (Hsu et al., 2007). While for all of the previous work it was difficult to obtained high NO_X removal efficiency, as it's for SO_X, thus, extra attention has been directed to NO_X. Nonetheless, there are several applicable absorbers, meanwhile, they represent one of the main elements in the reactor, and will directly be derived in the final byproducts (Choi, 2014; Mumford et al., 2012; Wei et al., 2012). Herein we applied a potassium source absorber that was KCl. Practically, the potassium content measured as K_2O and/or K content for that element, KCl is one of the highest among several candidates, such as MOP Potash, SOP Potash, KNO_3, etc., where KCl has 60–62.5 K_2O, and 49.8–51.9 K (GC Mgbeze, 2010; Hussain, 2015).

The whole previous work was only speaking about removing SO_X and NO_X, due to their harmful effects while spending a lot of money on it. We've put the cornerstone in opening a new direction of changing them into other useful products. Which were the complete fertilizer Nitrogen N Phosphorus P Potassium K (NPK), which was our main target to obtain from those toxic gases abatement. Furthermore, all the useful byproducts are sellable. While keep in mind using available and cheap equipment, to diminish the need for a giant fund to remove those gases, while getting benefits from the byproducts.

2. Material and methods

2.1. Materials

2.1.1. Chemical

Red phosphorus (purity of >99%), KCl (purity of >99%), deionize water, silica gel, cotton, H_2SO_3 (purity of >99%), SO_2, and NO gases (purity of >99%).

2.1.2. Tools

2.1.2.1. Yellow Phosphorus preparation. Alcohol burner, ring stand, test tubes and caps, clamp, water heater, bucket.

2.1.2.2. Gas testing. Gas analyzer, model Seitron C600, designed by Seitron Co., Italy. pH meter, model PHS-3E, designed by Shanghai INESA Scientific Instrument Co., Ltd., China. Deionized water. Stirrer. Buchner flask, model, SHUNU, GG-17, 1000 Ml, designed by Hangzhou Beibang Technology Co., Ltd. Digital heater magnetic stirrer mixer, model DF-101S, designed by Shanghai Yingdi Instrument Equipment Co., Ltd. O_3 generator. Two Ion Chromatography (I.C.) devices, model Thermo Scientific Dionex Aquion IC system and model Dionex DX-600, Designed by Thermo Fisher Scientific, USA, and Thermo Fisher Scientific, USA. X-ray diffractometer (XRD), model Rigaku, D / Max-2550 PC. Designed by, Rigaku, Tokyo Japan. RAMAN spectroscopy device. Modele inVia-Reflex, Designed by RENISHAW U.S.A.

2.2. Methods

2.2.1. White/Yellow phosphorus preparation method

Balance 1–5 g of the red phosphorus depending on the test tube specification, avoid the huge amount as the accumulated gas will increase the pressure and make it explodes, seal the test tube very good because white phosphorus will react with the oxygen, heat the test tube while it slides down in the horizontal axis (minus 10–30°), to force the gas to flow down and not to accumulate at the same place of the red phosphorus. At the same time cool down the gas side of the test tube with cooling water, avoid splashing the water on the hot side because it will make the test tube explode. After ensuring all the red phosphorus converted to white phosphorus, carefully heat all the test tube for a few seconds to liquefied all the white phosphorus (not important), transfer it to a hot water pool, and if necessary break the test tube. Cool down the water to solidify the White/Yellow phosphorus. Weigh the sample, typically the yield is 80–95%.

2.2.2. Gas removal process

The simultaneous removal of SO_X and NO_X was done for a bench-scale experiment. In the typical experiment we used 2900 ppm SO_2, and 550 ppm NO, they were bubbled in a 1L Buchner flask contains 1L deionize water, 30 g KCl, and 0.5 g yellow phosphorus (P_4). While the operating temperature was 55 °C, with vigorous stirring. The dust and moisture removal part contains cotton wools and silica gel respectively. Furthermore, the gas was measured continuously using the gas analyzer, while the pH and temperature were measured contentiously. A CFT-5G Ozone generator was used once for comparing the system efficiency with and without O_3. Whereas the solid content has been filtered and tested using RAMAN spectroscopy and XRD. On the other hand, the liquid was tested for the anions using the Thermo Scientific Dionex Aquion Ion Chromatography system uses 30 mM NaOH eluent, and for the cation using Dionex DX-600 uses 5 mM Methane sulfonic acid as eluent.

Further attention was given to NO_X, consequently, we also studied NO_X removal in bench-scale using 1L Buchner flask, 1L deionize water, 550 ppm NO, 0.5 g yellow phosphorus

(P_4), and 30 g KCl, while stirring magnetically and heating to 55 °C. In the meantime, the exhaust gas was measured using the gas analyzer, while the pH meter and the thermometer were for measuring the pH and temperature respectively. Additionally, the final P_4 ions and NO_2^-/NO_3^- were tested using a Dionex Aquion Ion Chromatography system.

Lastly, the reaction stoichiometry and effectiveness for NO and SO_2 removal were tested in a closed system. Typically, 1L three necks round bottom flask have been evacuated. Firstly, filled with NO. Secondly, with NO and H_2SO_3 as SO_2 carrier. Using 900 ml deionized water, 0.21 g P_4, 2 g KCl, the reaction stirred magnetically and carried out at 55 °C. The reaction tested regularly for 5 h using Ion Chromatography (see Fig. 1).

The removal efficiency for each of SO_X and NO_X was calculated as

$$\eta SOX = \frac{[(\boldsymbol{SO}2)1 - (\boldsymbol{SO}2)2]}{(\boldsymbol{SO}2)1} * 100 \tag{1}$$

$(SO_2)1$ = Input SO_2 ppm, $(SO_2)2$ = Exhaust SO_2 ppm obtained by the analyser.

ηSO_X = The process removal efficiency

$$\eta NOX = \frac{[(\boldsymbol{NO})1 - (\boldsymbol{NO})2]}{(\boldsymbol{NO})1} * 10 \tag{2}$$

(NO)1 = Input NO ppm, (NO)2 = Exhaust NO ppm obtained by the analyser.

ηNO_X = The process removal efficiency (Cheng, 2018; Liu and Chang, 1991; Liu and Chang, 1990).

3. Results and discussions

3.1. SO_X and NO_X simultaneously removal with and without O_3:

The simultaneous removal achieved using the conditions in Section 2.2.2 for the simultaneous removal, where the phosphorus slurry (P_4) actively oxidizes NO into one of the soluble forms N_XO_Y, which can be absorbed together with SO_2. To do so we applied KCl as an absorber, whereas P_4 has a low reaction rate with SO_2 (Liu and Chang, 1991; Chang, 1992) the absorber can do so and neutralize it. Furthermore, the oxygen is an important factor for the removal, because it will be converted to ozone when reacts with the phosphorus emulsion as in Eqs. (5)–(7) below. Besides, it will oxidize NO into one of the more soluble forms such as NO_2 or generally N_XO_Y. Meanwhile, we've tested the ozone O_3 effects on the removal process using an external ozone source, from Fig. 2 using the ozone we directly got 100% SO_X removal, and after 2 h for NO_X removal. Meantime, without the ozone existence, we can get it after 3 h. Thus, O_3 didn't have a huge difference, therefore, it will be an energy waste and will represent extra expenses (Liu and Chang, 1991).

In addition, a white fume formed, that depends on the oxygen content. It can damage the gas analyzer if didn't remove (Shuai Li, 2018). Thus we used the gas tail removing system for it, which contains silica gel and cotton wool. This fume resulted from the P_4 incomplete oxidation, it will decrease as the oxygen, the pH decline, and/or the ozone O_3 concentration increase, consistent with P_4 conversion to P_4O_6 or the more oxidized state of P_4O_{10}, then absorb the moisture to form H_2PO_2, H_2PO_3, and H_2PO_4 (Li et al., 2018).

Finally, about the NPK production claims, as we already have NO_2^-/NO_3^- they will spontaneously convert to NH_4^+ as the pH goes down, the medium is phosphorus which contains all the required phosphorus ions, and KCl has high potassium content, and will appear in the final products, that is clearly proving the production. Furthermore, all the Nitrogen N, Phosphorus P, and potassium K elements (NPK) fertilizer have been proved through the specified tests, either for the liquid ions, or for the solid precipitate, nonetheless, also their amount was identified. On the other hand, SO_X's existence will end up as K_2SO_4, which is also a rich potassium source. Fur-

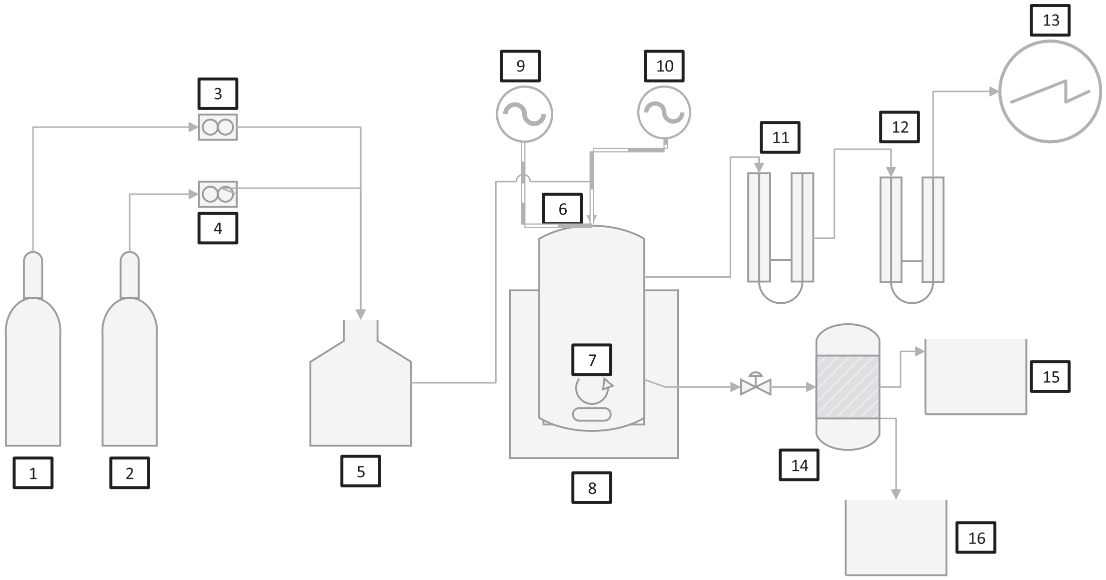

Fig. 1 Detailed experimental sections were; 1. SO_2, 2. NO, 3&4 Flowmeters, 5. Gas mixing tank, 6. Oxidation absorption reactor, 7. Stirrer, 8. Heating and stirring device, 9. pH meter, 10. Thermometer, 11. Silica gel in U tube, 12. Cotton in U tube, 13. Gas analyzer, 14. Separator, 15. Acids tank, 16. NPK elements.

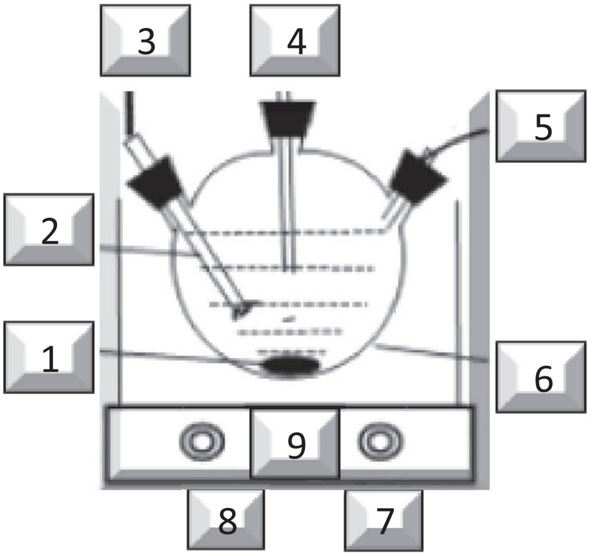

Fig. 2 Detailed close system experimental sections were; 1. Stirrer, 2. Solution emulsion, 3. Sample taking tube, 4. pH meter, 5. Thermometer, 6. 1L three necks round bottom flask as a reactor, 7. Reaction Temperature Controller, 8. Reaction Stirring Controller, 9. Heating and stirring device.

thermore, the extra produced acids are separated in a different tank, and the final NPK elements are extracted alone as final products in a different container (Jason C. Willett, 2004; Production and Use of Potassium, 1998).

Usually, the sulfur's emissions are treated either pre-combustion or by applying low sulfur emission compounds, which lead to minimizing the sulfur emissions, besides for SO_X removal it's easier to reach 100%, which makes the sulfur becomes a minor problem. On the other hand, for the Nitrogen Oxides NO_X has low solubility and high availability, thus, further tests were done focusing on NO_X removal investigation, and study the process feasibility under certain considerations.

3.2. Oxygen change with time:

For the previous P_4 studies they applied an increasing O_2 concentration of 4% to 20% that results in increasing NO_X removal efficiency, meanwhile, the white fume becomes lighter with the increase as the phosphorus reach the complete oxidation (Shih-Ger Chang, 1992; ShihGer Chang, 1994; Shuai Li, 2018). But none of them studied the practical oxygen consumption within the removal efficiency. Fig. 3 shows the oxygen change as the reaction goes with time, it was clear the oxygen is consuming as the reaction continues. The main factors affecting the oxygen are, the temperature, stirring, P_4 concentration, and the dispersion medium (Khoo, 2006). Whereas the oxygen consumed to produce the ozone (O_3), consequently, those factors will also affect the amount of the produced ozone production. Furthermore, the oxygen O_2 will be consumed to oxidize NO, and P_4, therefore, reduce the oxygen amount in the reactors. Moreover, K reacts with O_2 to produce potassium oxide K_2O, which is the main potassium source as fertilizer. While comparing SO_2 and NO simultaneous removal with only NO removal reveal that more oxygen is being consumed, resulting from the extra oxygen consumed to oxidize SO_2 to SO_3^{2-} and SO_4^{2-} as in Eqs. (20) and (21) or assist in converting it to H_2SO_4 (Li et al., 2014; Li et al., 2018) (see Fig. 4).

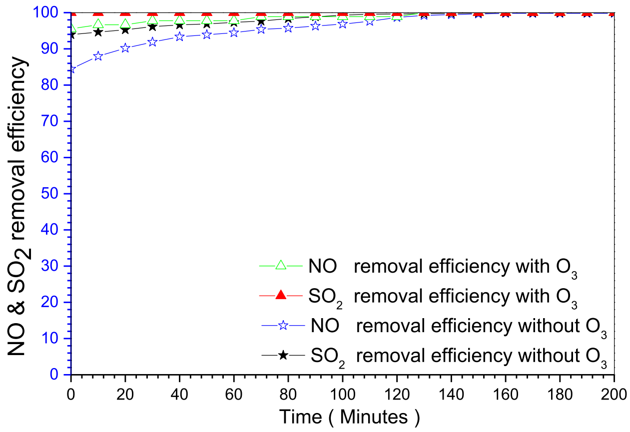

Fig. 3 SO_X and NO_X simultaneous removal with and without ozone.

3.3. Yellow phosphorus weight change effects

Likewise, in the literature it was reported from 0.25%w up to 3.5%w (Liu and Chang, 1991; Shih-Ger Chang, 1992; ShihGer Chang, 1994), accordingly was for small scale, herein we did for higher concentration. In a typical experiment, we add 0.125 g, 0.250 g, and 0.5 g of yellow phosphorus and 550 ppm NO in Buchner flask, contains 1L deionized water and 30 g of KCl, at 55^{O}C for 200 min, and 25 degrees at the stirring scale which is 1080 rpm (each scale is 43.33). After NO bubbled into the reactor a white mist formed, which is phosphoric acid that becomes denser as the stirring and temperature change. Additionally, it can be controlled by changing the pH and/or O_2 content of the reactor, meanwhile, only 10% to 15% can instantly be absorbed by the emulsion, and the remaining can be absorb using 40% to 60% concentrated phosphoric acid (Chang, 1992; Shih-Ger Chang, 1992; ShihGer Chang, 1994). Whereas for the specified case P_4 concentration consumed with time, thus NO_X removal efficiency. Nonetheless, the P_4 utilization rate is expressed using the P/N

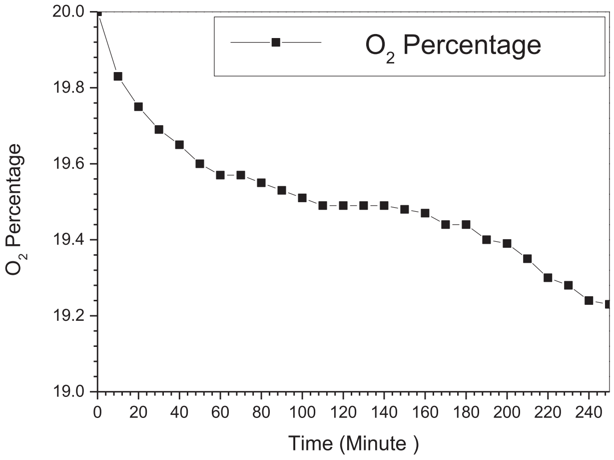

Fig. 4 Oxygen change for NO_X removal.

ratio as described below. From Fig. 5, it was clear as the P_4 weight increase NO_X removal efficiency will increase, this increase stated to the ozone generated due to the P_4 weight increase, then more NO is oxidized to NO_2 and become easier to absorb by the medium. Furthermore, increasing the P_4 weight, not only will increase the O_3 generation rate but will also guarantee a better mixing between P_4 and the NO_X, therefore, better removal efficiency (Liu and Chang, 1991; Pham & Chang, 1994).

3.4. Changing the emulsion stirring intensity effects

It was reported for a low impeller speed of 100 to 500 rpm, where the removal efficiency increased with the stirring increase, furthermore, increasing NO concentration for the same stirring intensity increases NO removal efficiency from 500 to 800 ppm (Hsu et al., 2007; Chang, 1992; Shuai Li, 2018). Herein, as it was for smaller intensity, we used higher intensity. Typically, we used 15, 25, and 35 degrees on the scale of the device (each degree on the scale equal to 43.33 rpm) which is equal to 650, 1083, and 1517 rpm. With 1L deionized water, 30g KCl, 0.5 g P_4, and 55 °C for 6.7 hrs. From Fig. 6, as the stirring intensity increase the removal efficiency increase, because, increasing the stirring intensity will raise the yellow phosphorus emulsion dispersion, additionally, it will increase the gas–liquid transfer rate, moreover, will increase the oxygen dispersion and holdup within the contact surface (Khoo, 2006). Meanwhile, the decrease stated to the increased interfacial area, thus, decreases the mass transfer resistance, besides the P_4 consumption (Hsu et al., 2007; Chang, 1992; Shuai Li, 2018).

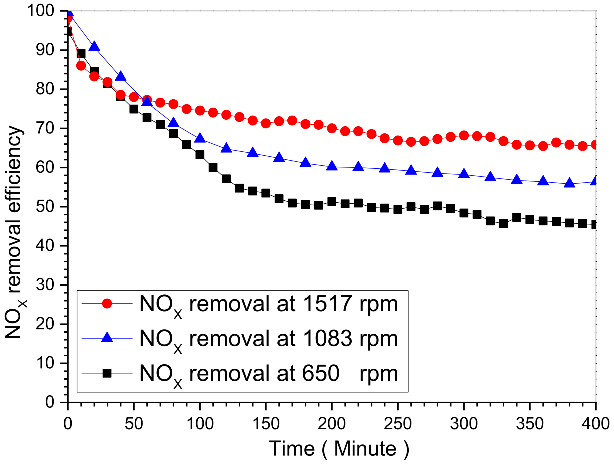

Fig. 6 NO_X removal efficiency as the stirring intensity change.

3.5. Emulsion temperatures differences

Most importantly the emulsion temperature, which is a critical factor for the removal efficiency, through controlling the O_3, whereas increasing the temperature from 45^{O}C to 65^{O}C increases O_3 concentration from 50 mg/m^3 to 280 mg/m^3, but have a reverse effect after this limit (Liu and Chang, 1991; Shuai Li, 2018). Although there are several studies, they were only for the maximum conditions, consequently, we investigated the changes in the removal efficiency when the temperature is constant during all the reactions. For this experiment, we used 1L deionized water, 0.5 g P_4, 550 ppm NO, and 30 g KCl, for different temperatures of 45 °C, 55 °C, and 65 °C. We can see from Fig. 7, NO_X removal efficiency depends on the emulsion temperature, as the temperature increases NO_X removal efficiency increases (Li et al., 2018). The removal efficiency for those temperatures was interestingly different, where NO_X removal efficiency decreased from the reaction beginning for the 45 °C, 55 °C, it was increasing for 65 °C, then sharply decreases due to the yellow phosphorus P_4 rapid consumption, which attributed to the increase in P_4 vapor concentration, then its shortage with the higher consumption rate. Meantime, the yellow phosphorus can spontaneously ignite at 85 °C or after it (Liu and Chang, 1990; Shuai Li, 2018), therefore, the main experiment was conducted at 55 °C for its stable removal efficiency. Furthermore, the elevated temperatures will consume the phosphorus content quickly and will make the ozone decompose and lost, besides, it will reduce NO gas solubility as it's inversely proportional to the temperature, nonetheless, it will increase the temperature will increase P_4 vapor concentration in the absorber (Wei et al., 2003; Wu et al., 2005).

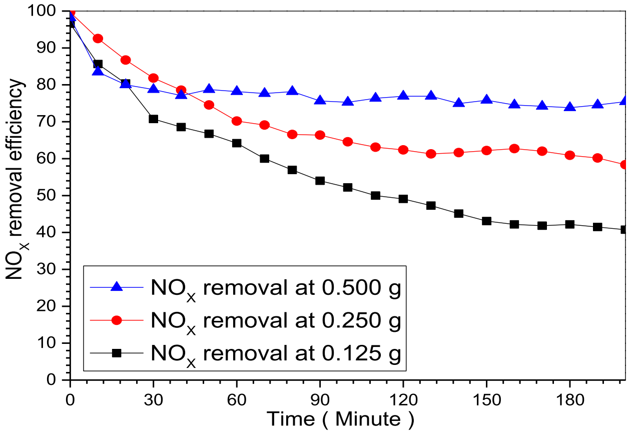

Fig. 5 Yellow phosphorus weight change effects on NO_X removal efficiency.

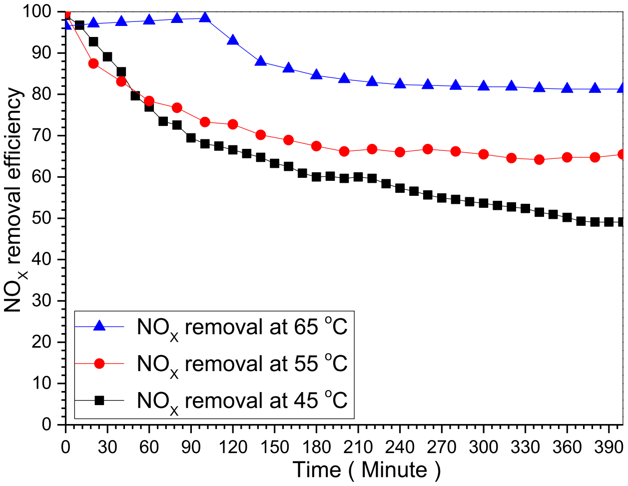

Fig. 7 NO_X removal efficiency as the emulsion temperature change.

3.6. The reaction pH effects

It was reported for 3, 7, and 9, where the removal was higher at low pH and continue, but after a longer time, it will reverse, where the higher will achieve lower removal efficiency (Liu and Chang, 1991; Liu and Chang, 1990; ShihGer Chang, 1994). Nevertheless, none have investigated the actual system, and pH change, herein we did for the actual experiment, using 1L deionized water, 550 ppm NO, 30 g KCl, 0.5 g P_4, and 55 °C. For the pH change effects on NO_X removal efficiency, it's clear from Fig. 8 the pH change lead to different NO_X removal efficiency. Where the pH change as the reaction goes with time, starting from the neutrality where the absorber has a higher ability for absorbing a higher amount of the acidic gases, thus has higher NO_X removal efficiency, or SO_X and NO_X simultaneous removal efficiency. This removal decrease with time as it becomes more acidic, due to the formed acids, which decrease the removal efficiency of the reaction goes with time, in order to achieve constant or a higher removal efficiency, an alkali may be added to change the pH toward more alkali, and also the reaction time. The pH change was different for the two cases of, only NO_X or the simultaneous SO_X and NO_X, due to the formation of sulfuric acid, together with the other acids in case of only NO including HCl, HNO_3, HNO_2, and H_3PO_4 (Nimmo, 2006; Song et al., 2003; Wei et al., 2003).

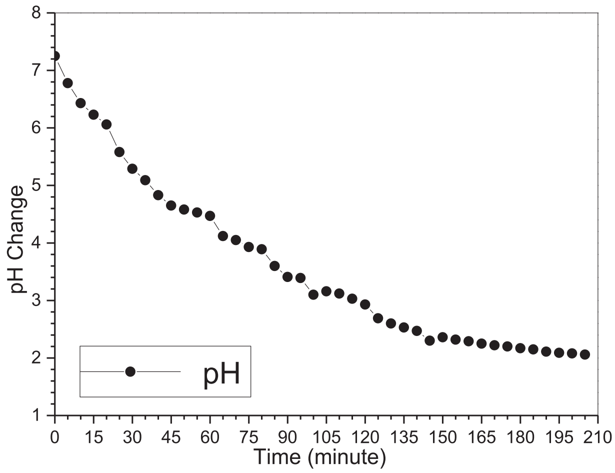

Fig. 8 pH change for NO_X removal.

3.7. Comparing NO_X removal using KCl with $CaCO_3$ and the phosphate rocks

We make a comparison for NO_X removal using our newly reported KCl with the most famous absorbers for the P_4 application, where were Calcium Carbonate and Phosphates Rocks (Wei et al., 2003; Wen, He, & Costello, 2002). Using 1L deionized water, 0.5 g yellow phosphorus, $55^{O}C$, 550 ppm NO, stirring for 1083 rpm, and 30g of KCl, 30g of phosphate rock, and 30g of $CaCO_3$. From Fig. 9 as we can see, $CaCO_3$ have stable NO_X removal at around 95%, followed by the phosphate rocks that decline at the early stage and become stable at around 85%, lastly, our KCl is also declined at the beginning and quickly stable around 80%. Whereas the reaction of NO and P_4 produces nitric acid and phosphoric acid, those acids react with the calcium carbonate to produce gypsum and other byproducts, which neutralize the medium and make it acceptable for more of the acidic gases NO_X. Thus, they have higher removal efficiency (Caillahua, 2018; Clamp, 2008; Dallas Burtraw, 2010). While the phosphate rocks contain some of the appetites like fluorapatite $Ca_5(PO_4)_3F$ and hydroxyapatites $Ca_5(PO_4)_3OH$ or $Ca_5(PO_4)_6(OH)_2$, P_2O_5, Minerals, and Oxides, which can do the same for the acids, better neutralize the generated acids (Azhar Hussain, 2015; Cheng, 2018; Renmin Li, 2018; Xinglei Zhao, 2009). Meantime, comparing the KCl, to several absorbers, they are either having lower removal efficiency, or if it was higher, it will be unstable removal efficiency, and quickly drop down, besides, if both are okay then it will be expensive. Nonetheless, here we can see KCl has 80% removal efficiency, stable for 5.3 hrs., and also has a very cheap price. Accordingly, it makes our detected KCl a very strong alternative for both, as well as for other available absorbers (Hsu et al., 2007; Khoo, 2006; ShihGer Chang, 1994; Song et al., 2003).

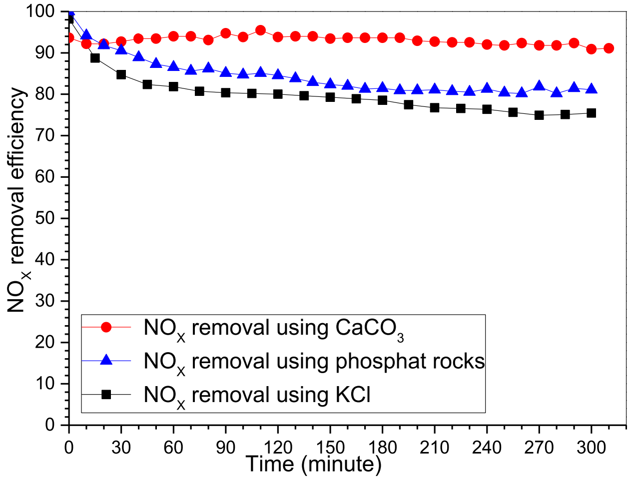

Fig. 9 Comparing NO_X removal using KCl with $CaCO_3$ and phosphate rock.

3.8. Reaction stoichiometry for only NO_X removal and SO_X and NO_X simultaneous removal

We investigate this process removal efficiency, and the P_4 utilization rate, using a close system experiment. Where we used 1L 3 necks rounded bottom flask contains 900 ml of deionized water, 0.2 g of P_4, 2.0 g of KCl, at $55^{O}C$, and 1083 rpm for 5 h, once with 500 ppm NO, and later using NO and 0.92 mM H_2SO_3 equal to 3000 ppm SO_2. We have tested the samples each 1 hr., using two Ion Chromatography (I.C.) described in section 2.2.2, Testing the emulsion seeking all the ions inside the system, whereas NO exist mainly as NO_2^- and smaller amount as NO_3^-. Also, P_4 exists as $H_2PO_2^-$, $H_2PO_3^-$, and commonly as $H_2PO_4^-$. While the sulfur exists as SO_3^{2-} and SO_4^{2-}. Additionally, for KCl together with the potassium ions, Cl^- ions were also clearly identified by the I.C., which reviled the separation of the two ions. Hence K is undergoing other reactions (Hsu et al., 2007; Shih-Ger Chang, 1992; Yunxiang Nie,

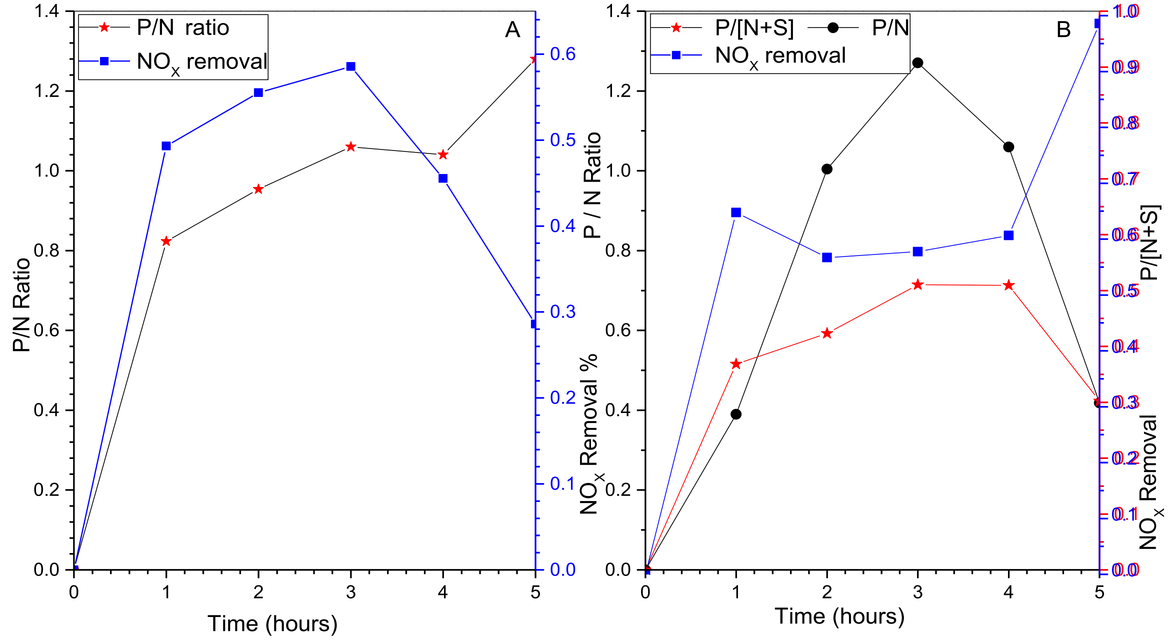

Fig. 10 (A) P/N for NO_X removal; (B) P/N + S for SO_X and NO_X removal, and NO_X removal change with time.

2018). Nevertheless, the other IC proved the K^+ and the NH_4^+, and the results are in Figs. 11–14 below.

Meanwhile, the efficiency and P_4 utilization investigated using P/N + S and P/N stoichiometric ratio, which represents the number of P mole required to remove 1 mol of N + S or only N. Which expressed by the;

$$P/N = ([H_2PO_2^-] + [H_2PO_3^-] + [H_2PO_4^-])/([NO_2^-] + [NO_3^-]) \quad (3)$$

$$P/N + S = ([H_2PO_2^-] + [H_2PO_3^-] + [H_2PO_4^-])/[([NO_2^-] + [NO_3^-]) + ([SO_3^-] + [SO_4^-])] \quad (4)$$

The main data plotted in Fig. 10, where P/N and P/N + S are shown during the actual removal process. Meantime, comparing the system differences with and without the SO_2 existence, reviled the P/N higher for NO_X removal alone and it

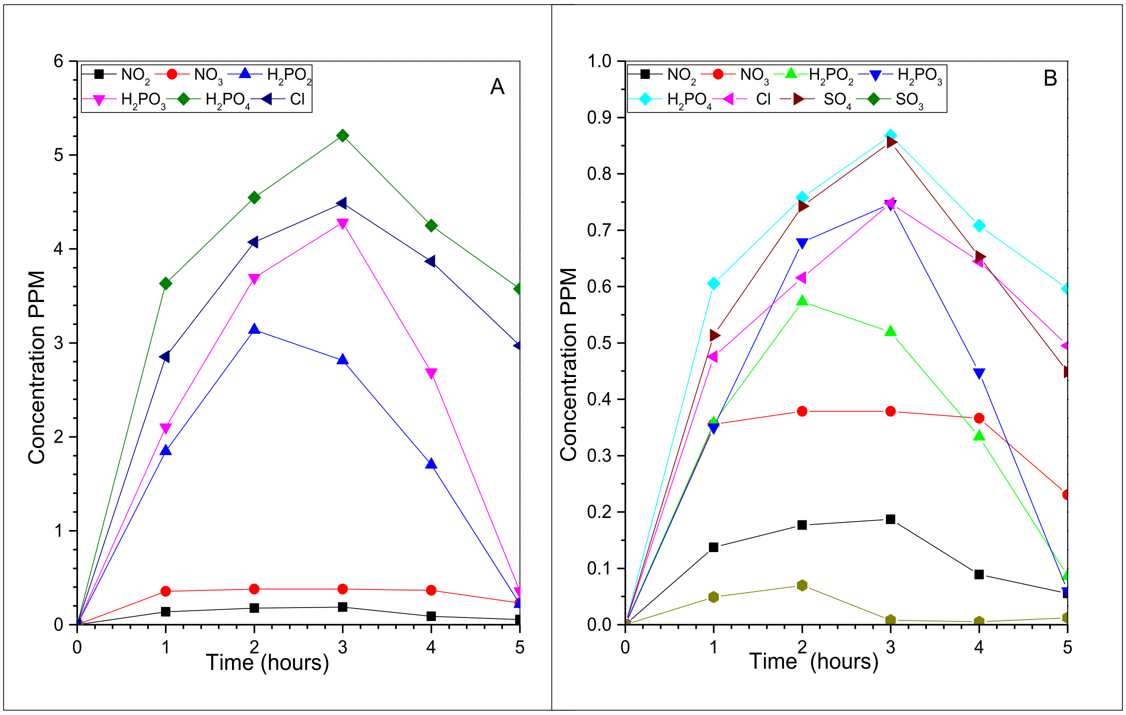

Fig. 11 Anions for (A) NO_X removal; and (B) SO_X and NO_X simultaneous removal.

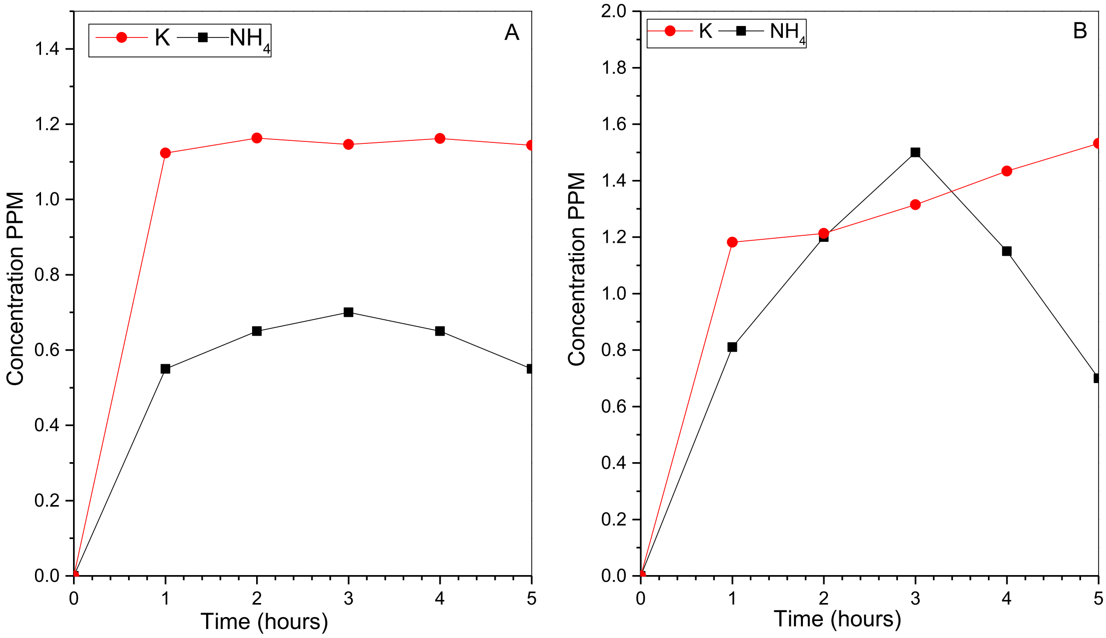

Fig. 12 Cations change for (A) SO_X and NO_X simultaneous removal, and (B) NO_X removal.

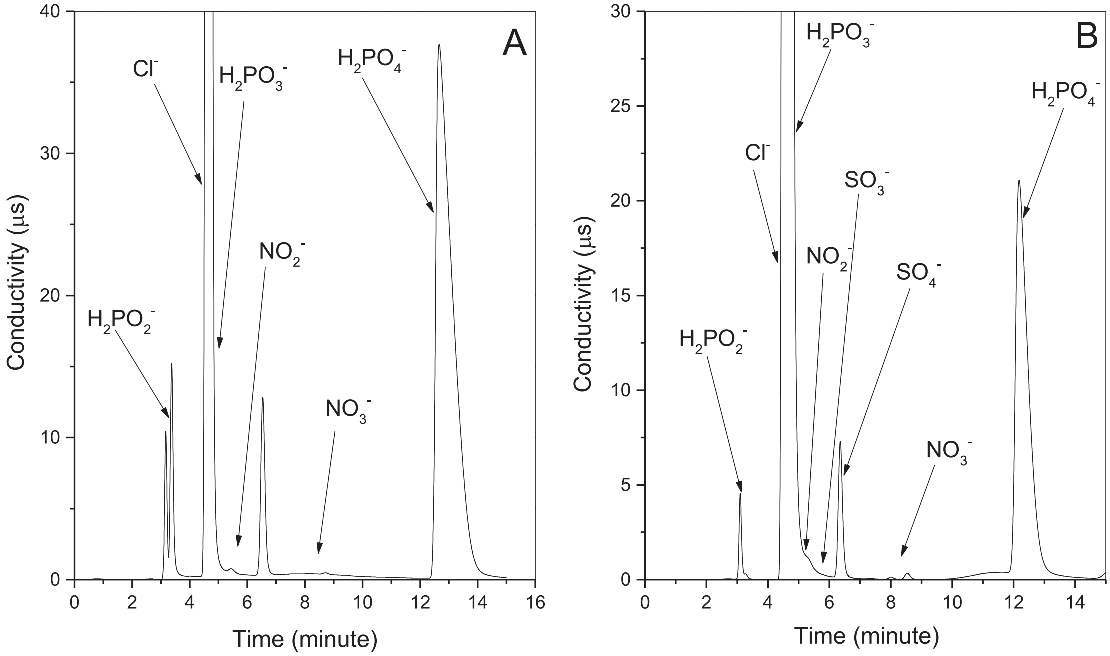

Fig. 13 I.C graph for the Anions for (A) NO_X removal; and (B) SO_X and NO_X simultaneous removal.

also continues to increase, while the simultaneous is increasing then decreasing. Moreover, the P/N stoichiometric ratio founded to be affected by the same factors affecting the NO_X removal including O_2, temperature, and P_4 weight. For instance, the oxygen existence results in complete oxidation and utilization of P_4, which will result in a lower P/N ratio. In addition, those temperatures, P_4 content, and O_2 concentration are affecting each other in opposite ways. Therefore, during the experiment, it's normally compromised between high NO_X removal efficiency or low P/N ratio. Typically, during the real operation, it's to obtaining higher NO_X removal efficiency while keeping a lower P/N ratio (Andrews, 1988; Pham and Chang, 1994; Chang, 1992).

Whereas, the P_4 amount will affect NO final products, when the P_4 amount is greater than NO, the majority of the products are in form of NO_3^- (Liu and Chang, 1990; Chang, 1992; Shih-Ger Chang, 1992), while if the P_4 amount is equal to or less than NO, the majority in form of NO_2^-. Meanwhile, the phosphorus ions are constant in the form of $H_2PO_4^- > H_2PO_3^- > H_2PO_2^-$ independent of P_4 amount. Additionally,

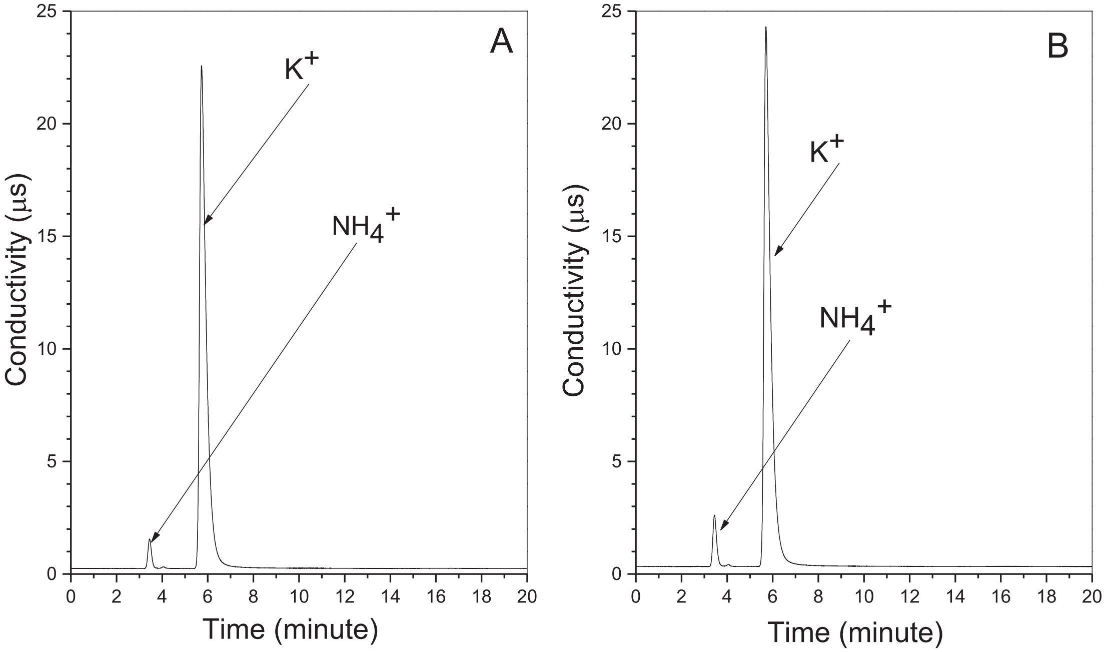

Fig. 14 I.C graph for the Cations for (A) SO_X and NO_X simultaneous removal; and (B) NO_X removal.

SO_2 was presented in the form of SO_4^{2-} and fewer amounts than SO_3^{2-} (Chang, and Lin, 1982). Nevertheless, as we used P_4 greater than NO, we've got more NO_3^- than NO_2^-, which can be seen in Fig. 11. Furthermore, the I.C. proves all those ions including $H_2PO_2^-$, $H_2PO_3^-$, $H_2PO_4^-$, NO_2^-, NO_3^-, SO_3^{2-} and SO_4^{2-}, as in Figs. 11–14 below.

In addition, for the simultaneous removal NO_X recovered as NO_2^- and NO_3^- represents ~50%, the rest are in form of several Nitrogen and Sulphur compounds (Liu and Chang, 1990; Chang, 1992; Shih-Ger Chang, 1992), with the majority in form of the Hydroxyimidodisulfate (HIDS) and imidodisulfate (IDS) at the slightly acidic environment, those HIDS and IDS compounds can be Hydrolyzed to NH_4^+ when the pH at around 2. The I.C. test for the cations in Figs. 12 and 14 has proved NH_4^+ existence, as it also proved the existence of potassium ions K^+. Lastly, the cations investigation has proven the latest element of the NPK complete fertilizer to exist within the final products, while for the solids it proved to have P_2O_5 and PO_4 that are part of P in the NPK fertilizer. As in the XRD and RAMAN spectroscopy describe below (Li, Loh, Matsushima, Nishioka, & Sadakata, 2002; Wen et al., 2002).

4. Solid precipitate investigation

4.1. Raman spectroscopy

Raman spectroscopy is a powerful technique for chemical structure identification, herein we investigated the solids precipitated crystals obtained from the reaction (using an inVia Raman microscope, designed by Renishaw in U.K.) as shown in Fig. 15, the main obvious peaks of the Raman bands were 360 cm^{-1}, 460 cm^{-1}, and 600 cm^{-1} that represent the majority and refer to the Phosphate PO_4, while a smaller amount exists at 1230 cm^{-1} in form of P_2O_5 crystals. It also indicates as the P_2O_5 is an intermediate state for the phosphorus oxidation it will finally stable at PO_4, thus represent the majority. However, both of them are rich phosphorus sources, while ammonia and potassium together with some other phosphorus are mainly in the liquid form (Lei Zhang, 2017; McManus 2012).

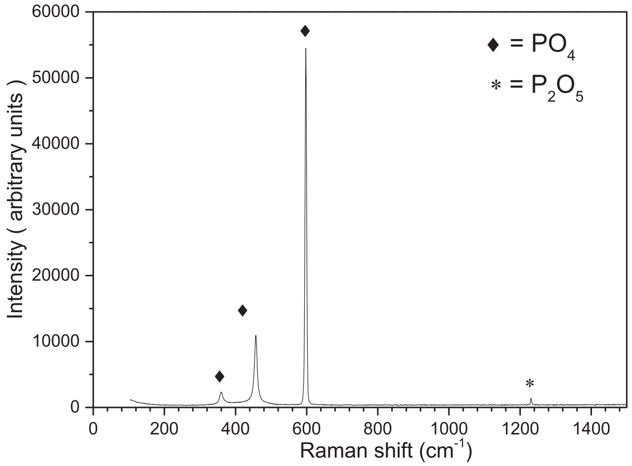

Fig. 15 RAMAN test for the solid precipitate.

4.1.1. XRD test

The morphology and microstructure of the solid precipitated samples were also investigated using X-Ray Diffractometer XRD (Rigaku, D/Max-2550 PC Tokyo Japan). The XRD spectra are shown in Fig. 16, where the peak at 2Θ = 21° the diffraction peak, represents the majority of the residue, which is assigned to the Phosphate PO_4 crystals. Additionally, the remaining peaks are minor and they represent a mixture of the Phosphate PO_4 and the Phosphorus pentoxide P_2O_5 and some amorphous, although several factors may affect the crystallinity, from all the experiments the precipitated crystals have

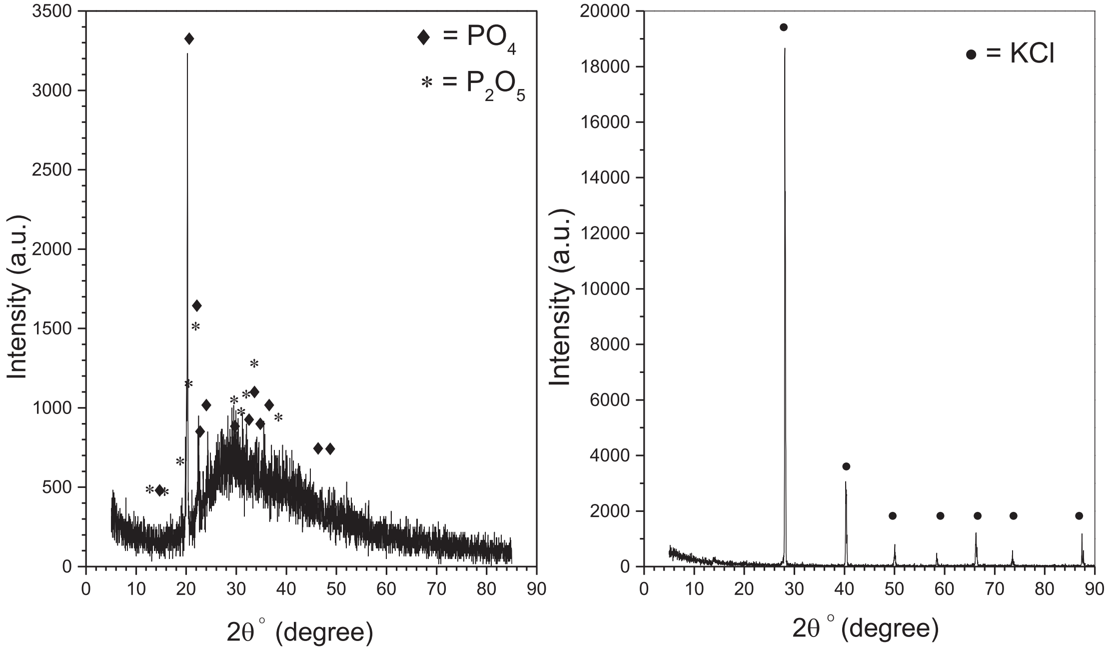

Fig. 16 XRD test for the solid precipitate.

almost the same size and white color. These results support that one of the Raman for the solid precipitates. Furthermore, it was compared with the XRD for the pure KCl that has shown beside it, where no peak was coexisting at the same peak (Kumar, 2007; Tea-Sung Kang, 2017).

4.2. Reaction mechanism of the process

The reaction of P_4 and O_2 can take place in both the aqueous phase and the gas phase. Whereas the liquid one occurs on the surface of the P_4 globule, hence will be affected by the reactor design, liquid/gas ratio, temperature, all the parameters that can change the dispersion of the melted phosphorus, and all the additives that may change the dielectric constant of the medium. On the other hand, the gas phase occurs between O_2 and the liberated P_4 from the emulsion at high temperatures (Bailar, 1973). The reaction between P_4 and O_2 produces O_3 and O atoms with an almost equal reaction rate. Where O_2 normally higher in the flue gas, thus O_3 production representing the main reaction path (Qian, 1995), the inferred equations are as following.

$$P_4 + O_2 \rightarrow P_4O + O \quad (5)$$

$$P_4O + nO_2 \rightarrow P_4O_{10} + mO \quad (6)$$

$$O + O_2 + M \rightarrow O_3 + M \quad (7)$$

M is another molecule that won't change during the reaction.

The basic reactions between the ozone and NO to produce the more soluble NO_2 will be affected by the oxidizing agent whether it was O or O_3. The produced NO_2 can react with NO to produce N_2O_3 or dimerize to N_2O_4.

$$NO + O_3 \rightarrow NO_2 + O_2 \quad (8)$$

$$NO + O + M \rightarrow NO_2 + M \quad (9)$$

$$NO + NO_2 + M \rightarrow N_2O_3 + M \quad (10)$$

$$NO_2 + NO_2 + M \rightarrow N_2O_4 + M \quad (11)$$

$$NO_2 + O_3 \rightarrow NO_3 + O_2 \quad (12)$$

$$NO + NO_3 \rightarrow 2NO_2 \quad (13)$$

$$NO_2 + NO_3 \rightarrow N_2O_5 \quad (14)$$

M is another molecule that won't change during the reaction.

The produced NO_2 and the other intermediates will form nitrous and nitric acid, by the direct reaction with water.

$$2NO_2 + H_2O \rightarrow HNO_3 + HNO_2 \quad (15)$$

$$N_2O_3 + H_2O \rightarrow 2HNO_2 \quad (16)$$

$$N_2O_4 + H_2O \rightarrow HNO_3 + HNO_2 \quad (17)$$

$$N_2O_5 + H_2O \rightarrow 2HNO_3 \quad (18)$$

$$2HNO_2 + O_2 \rightarrow 2HNO_3 \quad (19)$$

it's clear now why oxygen is important for the reactions, whereas it's required in most of the reactions. Additionally, increasing P_4 content will increase NO removal. While the phosphorus intermediate compound PO, PO_2, P_2O, and P_4O that result from P_4 and O_2 won't be shown up here (Andrews, 1988; H. Cordes, 1965).

If SO_X is added as SO_2, the reaction mechanism is as the following (Christopher H. Nelli, 1998; David Littlejohn, 1986; Jetawattana, Spring 2005; Anglada, 2019).

$$2SO_2 + O_2 \rightarrow 2SO_3 \quad (20)$$

$$2SO_3 + O_2 \rightarrow 2SO_4 \quad (21)$$

$$SO_4 + 2H_2O + 2M \rightarrow H_2SO_4 + 2MOH \quad (22)$$

$$SO_3 + H_2O \rightarrow H_2SO_4 \quad (23)$$

$$SO_2 + H_2O \rightarrow H_2SO_3 \quad (24)$$

$$2H_2SO_3 + 2H_2O + 2M \rightarrow 2H_2SO_4 + 2H_2M \quad (25)$$

M is another molecule that won't change during the reaction.

In fact, the majority is found to occur through the NO/SO_2 producing HADS, which is generally expressed as Eq. (26):

$$NO_2 + SO_3^{2-}/HSO_3^{-} \rightarrow NO_2^{-} + SO_3^{-}/HSO_3 \quad (26)$$

Actually, the existence of SO_3^-/HSO_3 in greater than 1 mM can derive reaction (26) to occur, which is typically happening as the following (David Littlejohn, 1986; Anglada, 2019).

$$NO_2^{-} + 2HSO_3^{-} \rightarrow HON(SO_3)_2^{2-} + OH^{-} \quad (27)$$

Nevertheless, the HADS goes through sulfonation and/or hydrolysis to form N-S compounds, the overall reactions can be summarized as the following:

$$NO_2^{-} + 3HSO_3^{-} + H_2O \rightarrow NH_4^{+} + SO_4^{2-} + H^{+} \quad (28)$$

The removal process is mainly done by KCl, which will react with the final products from all of the above reaction, as follows:

$$KCl + HNO_3 \rightarrow KNO_3 + HCl \quad (29)$$

$$KCl + H_2SO_4 \rightarrow K_2SO_4 + 2HCl \quad (30)$$

Finally, the reaction of nitric acid and KCl will produce KNO_3 if only NO was added or KNO_3 and K_2SO_4 if the SO_2 and NO were added together, KNO_3 is a source of potassium for fertilizer which contain 44% K_2O and 36.5% K. Meanwhile, if SO_2 is presented then we will get H_2SO_4 and thus finally we will obtain K_2SO_4 which also contains 50–52 K_2O and 41.5–43.2 K (Liu et al., 2001; Production and Use of Potassium, 1998; Wei et al., 2003; Wen et al., 2002).

5. Conclusion

In the present study, we investigated SO_X and NO_X simultaneous removal, and the possibility to obtain the complete fertilizer NPK, using the yellow phosphorus P_4 and KCl.

After series of optimization experiments, the removal efficiency under the optimum conditions of a temperature of 55 °C, P_4 weight of 0.5 g, stirring intensity of 1083 rpm, and varying O_2 and pH, where the simultaneous removal for 550 ppm NO_X and 2900 ppm of SO_X reach 100% in 2 hrs. using O_3, and after 3 hrs. without it. Nevertheless, comparing to the most famous two absorbers, revile it's the best available alternative for both and the strongest competitor. Meantime, the IC proved all the claimed ions quantitatively and qualitatively, therefore, indicates all the NPK ions and confirms their existence. Besides, the inferred reaction mechanism. And finally, the solid investigation proves the precipitated crystals are rich in phosphorus ions.

Declaration of Competing Interest

The authors declare that they have no known competing financial interests or personal relationships that could have appeared to influence the work reported in this paper.

Acknowledgment

Funding: This work was supported by the National Natural Science Foundation of China [U1660107].

References:

Andrews, L.W., Robert, 1988. Matrix reactions of oxygen atoms with P_4 Infrared spectra of P_4O, P_2O, PO and PO_2. J. Am. Chem. Soc. 110 (17), 5605–5611.

Azhar Hussain, M.A., Ahmad, Hafiz, Nazir, Qudsia, Mustafa, Ayesha, Afzal, Alii, Zeb, Hassan, 2015. Comparative effectiveness of SOP and MOP for crop productivity in Pakistani soils. Int. J. Agron. Agric. Res. (IJAAR) 6, 256–267.

Caillahua, M.C.M., José, Francisco, 2018. Technical feasibility for use of FGD gypsum as an additive setting time retarder for Portland cement. J. Mater. Res. Technol. 7 (2), 190–197.

Cheng, G.Z., Chuanxiang, 2018. Desulfurization and denitrification technologies of coal-fired flue gas. Polish J. Environ. Stud. 27 (2), 481–489. https://doi.org/10.15244/pjoes/75959.

Choi, J.L., Choi, Kang Soo, Kim, Dong Yun, Kim, Yong Jin, Soo, Sang, 2014. Dry De-NOx process via gas Phase photochemical oxidation using an ultraviolet and aerosolized H_2O/H_2O_2 Hybrid System. Energy Fuels 28 (8), 5270–5276. https://doi.org/10.1021/ef500645a.

Christopher H. Nelli, G. T. R. (1998). Simultaneous sulfur dioxide and nitrogen dioxide removal by calcium hydroxide and calcium silicate solids. J. Air Waste Manage. Assoc. 48(9), 819-828. doi:10.1080/10473289.1998.10463728.

Clamp, F. (2008). Trials for the use of recycled gypsum in cement manufacture. Project code: PBD022-001, Jacobs Engineering UK Limited.

Dallas Burtraw, S.J., Szambelan. (2010). US emissions trading markets for SO2 and NOx.: New York: Routledge.

Liu, D.K., Chang, S.G., 1991. Removal of NOx and SO2 from flue gas using aqueous emulsions of yellow phosphorus and alkali. Environ. Sci. Technol. Res. 25(1), 55–60.

David Littlejohn, K.Y.H., Chang, S.G., 1986. Kinetics of the reaction of nitric oxide with sulfite and bisulfite ions in aqueous solution. Inorg. Chem. 25 (18), 3131–3135. https://doi.org/10.1021/ic00238a007.

GC Mgbeze, Y.A., 2010. The effects of NPK and farm yard manure on the growth and development of the African yam bean (Sphenostylis stenocarpa Hochst ex. a rich). African Journal of Biotechnology., 9 (37), 6085-6090

H. Cordes, W.W., 1965. Einige aussagen zur oxydation des phosphors. Zeitschrift für Physikalische Chemie., 46(1-2), 35–48.

Hsu, H.W., Chou, K.S., Lu, C.L., 2007. Performance characteristics of NOx removal by aqueous emulsions of yellow phosphorus. Chem. Eng. Commun. 177(1), 105–120. doi: 10.1080/00986440008912163.

Hussain, A. A., Muhammad Ahmad, Hafiz Tanvir Nazir, Qudsia Mustafa, Ayesha Afzal, Ali Zeb, Hassan, 2015. Comparative effectiveness of SOP and MOP for crop productivity in Pakistani soils-A review. Int. J. Agron. Agric. Res. (IJAAR), 6(4), 256–267.

Jason C. Willett, J.M.K., Linder Roberts, 2004. POTASH. POTASH, 11.

Jetawattana, S., 2005. Sulfur dioxide, source of (bi)sulfite. The University of Iowa, Iowa City, IA 52242-1181, 77, 222, 11.

John C. Bailar, A. F. T. D. (1973). Comprehensive inorganic chemistry. Oxford: Pergamon press; distributed by compendium publishers, Elmsford, N.Y.

Josep M. Anglada, M. T. C. M.-C., Joseph S. Francisco and Manuel F. Ruiz-López. (2019). Triplet state promoted reaction of SO2 with H2O by competition between proton coupled electron transfer (pcet) and hydrogen atom transfer (hat) processes. Physical Chemistry Chemical Physics, 19, 9779-9784. doi:10.1039/C9CP01105F.

Joseph Alcamo, M. A., Jean-Paul Hettelingh, Maria Holmberg, Leen Hordijk, Juha Kämäri, Lea Kauppi, Pekka Kauppi, Gabor Kornai, Annikki Mäkelä. . (1987). Acidification in Europe: a simulation model for evaluating control strategies. Jornal Ambio, 232-245.

Khoo, H.H.T., Reginald, B.H., 2006. Environmental Impact Evaluation of Conventional Fossil Fuel Production (Oil and Natural Gas) and Enhanced Resource Recovery with Potential CO2 Sequestration. Energy Fuels 20 (5), 1914–1924. https://doi.org/10.1021/ef060075+.

Kumar, J. S. T. a. B. (2007). Water Durable Lithium Ion Conducting Composite Membranes from the Li2O - Al2O3 - TiO2 - P2O5 Glass-Ceramic. J. Electrochem. Soc, 154(4).

Lei Zhang , L. C., Lai shi Zhao, Thomas J. Algeo, Zhong-Qiang Chen, Zhi hong Li, Zheng yi Lv, Xiang dong Wang. (1 August 2017). Raman spectral, elemental, crystallinity, and oxygen-isotope variations in conodont apatite during diagenesis. Geochimica et Cosmochimica Acta, 210, 184–207.

Li, Q., Wang, X., Xin, Y., Zhang, Z., Zhang, Y., Hao, C., Zheng, L., 2014. A unified intermediate and mechanism for soot combustion on potassium-supported oxides. Sci. Rep. 4, 4725. https://doi.org/10.1038/srep04725.

Li, S. Y., Jiaqiang Wang, Chi Xie, Delong Luo, Yongming Li, Kai He, Dedong Mei, Yi. (2018). Removal of NOx from flue gas Using yellow phosphorus and phosphate slurry as adsorbent. Energy & Fuels, 32(4), 5279 -5288. doi:10.1021/acs.energyfuels.7b03964.

Li, Y., Loh, B.C., Matsushima, N., Nishioka, M., Sadakata, M., 2002. Chain Reaction Mechanism by NOx in SO2 Removal Process. Energy Fuels 16 (1), 155–160. https://doi.org/10.1021/ef0101309.

Lindsay. L. McManus , F. B., George. A. Burke , Brian. J. Meenan , Adrian. R. Boyd and Hugh. J. Byrne (2012). Assessment of an Osteoblast-like Cell Line as a Model for Human Primary Osteoblasts Using Raman Spectroscopy. Dublin Institute of Technology DIT Biophotonics and Imaging, 137(7), 1559–1569.

Liu, H., Katagiri, S., Okazaki, K., 2001. Drastic SOx Removal and Influences of Various Factors in O2/CO2 Pulverized Coal Combustion System. Energy Fuels 15 (2), 403–412. https://doi.org/10.1021/ef000171p.

Liu, D.K., Chang, S.G., 1990. Removal of nitrogen and sulpher oxides from waste gases using a phosphorus/alkali emulsion. Nature, 343, 151–153.

Mumford, K.A., Smith, K.H., Anderson, C.J., Shen, S., Tao, W., Suryaputradinata, Y.A., Stevens, G.W., 2012. Post-combustion Capture of CO2: Results from the Solvent Absorption Capture Plant at Hazelwood Power Station Using Potassium Carbonate Solvent. Energy Fuels 26 (1), 138–146. https://doi.org/10.1021/ef201192n.

Nimmo, W. P., A. A. Williams, P. T. (2006). Enhanced NOx Reduction with SO2 Capture under Air-Staged Conditions by Calcium Magnesium Acetate in an Oil-Fired Tunnel Furnace. Energy & Fuels, 20(5), 1879-1885. doi:10.1021/ef060011z.

Pham, E.K., Chang, S.-G., 1994. Removal of NO from flue gases by absorption to an iron(ii) thiochelate complex and subsequent reduction to ammonia. Nature 369 (6476), 139–141. https://doi.org/10.1038/369139a0.

Production and Use of Potassium. (1998). Better Crops, 82, 6–8.

Qian, H.-B.D., Hamilton, Paul B., Peter, A., 1995. High-resolution spectroscopic study of the oxidation of white phosphorus. J. Chem. Soc., Faraday Trans. 91 (18), 2993–2998. https://doi.org/10.1039/FT9959102993.

Renmin Li, T.L., Zhang, Yimin, Huang, Jing, 2018. Mechanism of novel K_2SO_4/KCl composite roasting additive for strengthening vanadium extraction from vanadium–titanium magnetite concentrate. Minerals. 8 (426), 11. https://doi.org/10.3390/min8100426.

S. G. Chang, D. L., and N. H. Lin. (July 1, 1982). Kinetics of Reactions in a Wet Flue Gas Simultaneous Desulfurization and Denitrification System. Flue Gas Desulfurization, 188, 127–152.

S. G. Chang, G. C. L. (1992). LBL PhoSNOX process for combined removal of SO2 and NO from flue gas. Environmental Progress., 11 (1), 8.

Shih-Ger Chang, E. C. D. K. L., San Pablo, both of Calif. (1992). U.A. Patent No. 5,106,601. U. S. Patents.

ShihGer Chang, E. C., Calif. (1994). United States Patent No. 5,348,715. U. S. Patents.

Shuai Li, J. Y., Chi Wang, Delong Xie, Yongming Luo, Kai Li, He, Dedong Mei, Yi. (2018). Removal of NOx from flue gas using yellow phosphorus and phosphate slurry as adsorbent. Energy & Fuels, 32(4), 5279-5288. doi:10.1021/acs.energyfuels.7b03964.

Song, Q., Shibamori, Y., Sadakata, M., Koshi, M., 2003. Research on Homogeneous Oxidation of NO and SO2 in Flue Gas by Chain Reactions. Energy Fuels 17 (6), 1549–1553. https://doi.org/10.1021/ef0340209.

Susan M. Bernard, J. M. S., Anne Grambsch, Kristie L. Ebi., Isabelle Romieu. (2001). The potential impacts of climate variability and change on air pollution-related health effects in the United States. Journal Environmental health perspectives, 109(suppl 2), 199–209.

Tea-Sung Kang, S.-J. L. (2017). Fabrication of Calcium Phosphate Glass Using Eggshell and its Crystallization Behavior. J. Korean Ceram. Soc., 54.

Wei, X., Guo, X., Li, S., Han, X., Schnell, U., Scheffknecht, G., Risio, B., 2012. Detailed Modeling of NOx and SOx Formation in Co-combustion of Coal and Biomass with Reduced Kinetics. Energy Fuels 26 (6), 3117–3124. https://doi.org/10.1021/ef201729r.

Wei, X., Han, X., Schnell, U., Maier, J., Wörner, H., Hein, K.R.G., 2003. The Effect of HCl and SO2 on NOx Formation in Coal Flames. Energy Fuels 17 (5), 1392–1398. https://doi.org/10.1021/ef030010w.

Wen, B., He, M., Costello, C., 2002. Simultaneous Catalytic Removal of NOx, SOx, and CO from FCC Regenerator. Energy Fuels 16 (5), 1048–1053. https://doi.org/10.1021/ef010268r.

Wu, Z.L., Gao, X., Luo, Z.Y., Wei, E.Z., Zhang, Y.S., Zhang, J.Z., Cen, K.F., 2005. NOx Treatment by DC Corona Radical Shower with Different Geometric Nozzle Electrodes. Energy Fuels 19 (6), 2279–2286. https://doi.org/10.1021/ef0400823.

Xinglei Zhao, M.A.S., Smith, Kathryn H., Kentish, Sandra E., Fei, Weiyang, Stevens, Geoffrey W., 2009. Study on the interaction between NOx and K_2CO_3 during CO_2 absorption. Energy Fuels 23, 6. https://doi.org/10.1021/ef9001082.

Yunxiang Nie, S.L., Chunjin, Wu., Wang, Chi, He, Dedong, Mei, Yi, 2018. Efficient removal of SO_2 from flue gas with phosphate rock slurry and Investigation of reaction mechanism. Ind. Eng. Chem. Res.